ORIGINAL ARTICLE

Plant, Cell & Environment | PCE WILEY

The maize shoot ionome: Its interaction partners, predictive power, and genetic determinants

Benjamin Stich[1,2,3] | Andreas Benke[3] | Maria Schmidt[1] | Claude Urbany[3] | Rongli Shi[4] | Nicolaus von Wirén[4]

[1]Institute for Quantitative Genetics and Genomics of Plants, Heinrich Heine University, Düsseldorf, Germany

[2]Cluster of Excellence on Plant Sciences, Düsseldorf, Germany

[3]Max Planck Institute for Plant Breeding Research, Köln, Germany

[4]Leibniz Institute of Plant Genetics and Crop Plant Research, Gatersleben, Germany

Correspondence
Benjamin Stich, Institute for Quantitative Genetics and Genomics of Plants, Heinrich Heine University, 40225 Düsseldorf, Germany.
Email: benjamin.stich@hhu.de

Present address
Andreas Benke, Strube Research GmbH & Co. KG, Hauptstraße 1, 38387 Söllingen, Germany.

Claude Urbany, KWS Saat SE, Grimsehlstr. 31, 37555 Einbeck, Germany.

Abstract

An improved understanding of how to manipulate the accumulation and enrichment of mineral elements in aboveground plant tissues holds promise for future resource efficient and sustainable crop production. The objectives of this study were to (a) evaluate the influence of Fe regimes on mineral element concentrations and contents in the maize shoot as well as their correlations, (b) examine the predictive ability of physiological and morphological traits of individual genotypes of the IBM population from the concentration of mineral elements, and (c) identify genetic factors influencing the mineral element composition within and across Fe regimes. We evaluated the concentration and content of 12 mineral elements in shoots of the IBM population grown in sufficient and deficient Fe regimes and found for almost all mineral elements a significant (α = 0.05) genotypic variance. Across all mineral elements, the variance of genotype*Fe regime interactions was on average even more pronounced. High prediction abilities indicated that mineral elements are powerful predictors of morphological and physiological traits. Furthermore, our results suggest that ZmHMA2/3 and ZmMOT1 are major players in the natural genetic variation of Cd and Mo concentrations and contents of maize shoots, respectively.

KEYWORDS

genomic prediction, ionomic prediction, iron regime, maize, physiological and morphological traits, QTL mapping, shoot ionome

1 | INTRODUCTION

A better understanding of processes and genes regulating mineral element uptake and how to manipulate the concentrations of mineral elements in aboveground plant tissues holds promise for future resource-efficient and sustainable crop production (Stein et al., 2017) as well as for bio-fortification towards alleviating global malnutrition (http://www.harvestzinc.org/harvestplus). Studies on the composition of plant mineral elements are referred to as ionomics (Lahner et al., 2003). Their aim is to reveal knowledge about the networks controlling uptake, transport, and accumulation of mineral elements. Ionomic profiling is amenable to high-throughput phenotyping, which when coupled with quantitative genetic approaches such as quantitative trait locus (QTL) mapping or genome wide association studies becomes a powerful tool for gene discovery (Baxter, Gustin, Settles, & Hoekenga, 2013).

The majority of such studies has been performed in model plants (e.g. Bentsink, Yuan, Koornneef, & Vreugdenhil, 2003; Ghandilyan et al., 2009; Klein & Grusak, 2009; Salt, Baxter, & Lahner, 2008; Vreugdenhil, Aarts, Koornneef, Nelissen, & Ernst, 2004; Waters &

Grusak, 2008). Only a few studies have performed genetic analyses of the ionome of crop plants such as bean (Blair, Astudillo, Grusak, Graham, & Beebe, 2009), rice (Stangoulis, Huynh, Welch, Choi, & Graham, 2007), Sorghum (Shakoor et al., 2016), or rapeseed (Bus et al., 2014). Two studies used a quantitative genetic approach to dissect the ionome of maize grains using the intermated B73 x Mo17 (IBM) population (Asaro et al., 2016; Baxter et al., 2013). Baxter et al. (2013) described 25 QTL for grain concentrations of nine mineral elements that were detected as significant in two or more locations and, thus, were suggested as targets for biofortification programs. In the study of Asaro et al. (2016), which comprised additional environments to those sampled by Baxter et al. (2013), a total of 79 QTL controlling seed elemental accumulation were detected when each environment was analysed separately. While a set of these QTL was found in multiple environments, the majority were specific to a single environment, illustrating the importance of genotype*environment interactions. Similar results were obtained with segregating populations different from IBM (Gu et al., 2015; Simić et al., 2012). However, despite the important role of the mineral elements during the vegetative development of plants, no earlier study examined the inheritance of the shoot ionome of a C4 species.

Most previous studies examined the concentration of mineral elements. Mineral element concentrations reflect primarily the nutritional status of a plant or tissue and provide valuable information on differences in uptake, metabolism, or allocation among genotypes as long as biomass differences between genotypes are low. In our study, we considered additionally mineral element contents, that is, the product of concentration and biomass. These shoot contents reflect the cumulative nutrient uptake and translocation under consideration of the growth response.

The plant's ionomic state results from an interaction between the genotype and the environment, where the latter is strongly influenced by the soil (Baxter et al., 2012). However, our present knowledge of these complex genotype*environment interactions remains sketchy and limited in particular by the vast and discontinuous variation in soil composition at multiple scales in nature (Stein et al., 2017). Joint collections of both plant accessions and adjacent soil were suggested to overcome this bottleneck (Baxter et al., 2012). Apart from being laborious, disadvantages of such approaches are that in most cases the experimental design does not allow to separate genotype*environment interaction variance from error variance. Furthermore, it is impossible to dissect genotype*environment interactions into genotype*individual mineral element interactions. Therefore, such studies need to be complemented by experiments with artificial growth media, in which nutrient supplies can be controlled. However, such studies are lacking so far.

Iron is one essential mineral element, required for many important biochemical processes, including photosynthesis and respiration, where it participates in electron transport (Marschner, 2012). Therefore, we have chosen Fe exemplarily as the factor to be altered in a hydroponic culture to study a specific form of genotype*environment interaction, the genotype*Fe regime interaction, and to identify the underlying genetic factors.

In agricultural research (Bej & Basak, 2014) and especially plant breeding (Wallace, Rodgers-Melnick, & Buckler, 2018), a high interest exists in exploiting biomolecular signatures to predict complex phenotypes. Baxter et al. (2008) have demonstrated that shoot ionomic signatures in one *Arabidopsis thaliana* genotype can be used to identify plants that experience an environmental cue. However, to the best of our knowledge, the accuracy of such approaches has not been reported for segregating populations, that is, for entries that differ in their genetic make-up. Furthermore, only few studies have evaluated up to now the predictive ability of mineral elements to estimate genotypic differences in other physiological or molecular traits.

The objectives of this study were to (a) evaluate the influence of Fe regimes on mineral element concentrations and contents in the maize shoot as well as their correlations, (b) examine the ability of predicting an environmental perturbation from the ionomic response across a segregating population, (c) examine the predictive ability of physiological and morphological traits of individual genotypes of the IBM population from 110 the concentration of mineral elements, and (d) identify genetic factors influencing 111 the mineral element concentrations or contents within and across Fe regimes.

2 | MATERIALS AND METHODS

2.1 | Plant material

The recombinant inbred lines (RIL) of the intermated B73 x Mo17 (IBM) syn4 population (Lee et al., 2002) were examined in the current study. Due to the unavailability of seeds for the RIL MO040, MO043, MO048, MO057, MO062, MO063, MO076, MO079, and MO344, a total of 85 RIL were evaluated.

2.2 | Culture conditions and measured mineral elements

Maize seeds were sterilized in a 3% NaClO solution for 3 min and then treated with $60°C$ hot water for 5 min (Benke et al., 2014). Afterwards, seeds were placed between two filter paper sheets moistened with saturated $CaSO_4$ solution for germination in the dark at room temperature. After 6 days, the germinated seeds were transplanted to a continuously aerated nutrient solution with element concentrations as described by von Wiren, Marschner, and Römheld (1996). The plants were supplied with 100 μM Fe(III)-EDTA for 7 days. From day 14–28, plants were supplied with 300 (Fe sufficient) (Urbany et al., 2013) or 10 (Fe deficient) (Shi et al., 2018) μM Fe(III)-EDTA. The nutrient solution was renewed every third day. Plants were cultivated from day 7 to day 28 in a growth chamber at a relative humidity of 60%, a light intensity of 170 $\mu mol \ m^{-2} \ s^{-1}$ in the leaf canopy, and a day-night temperature regime of 16 hr/$24°C$ and 8 hr/$22°C$, respectively. Four plants of each RIL were grown in one shaded 5 L pot. Two separate pots were used for the two examined Fe concentrations ($T = 2$). All pots were arranged in a growth chamber following a

split-plot design, where the two parental inbreds were included as controls. The entire experiment was replicated R = 3 times. For each RIL, the shoot of the four plants from one pot were pooled so that each RIL was represented by one sample for each of the three replicates in each of the two Fe regimes. Afterwards, the entire sample was ground and the concentrations of 12 mineral elements (Figure 1) were measured using inductively coupled plasma optical emission spectrometry (ICP-OES, iCAP 6,400, Thermo Fisher) according to Shi et al. (2012). In a previous study, the variation of morphological and physiological traits of the same experiment has been reported (Benke et al., 2014).

2.3 | Statistical analyses

Upon the removal of outliers with residuals larger than 2.5 times the standard deviation of the residuals, the concentrations of each mineral element were analysed across both Fe regimes using the following mixed model:

$$y_{ijk} = \mu + g_i + t_j + g_i * t_j + r_k + e_{ijk},$$

where y_{ijk} was the observed elemental concentration of the ith genotype in the pot of the jth Fe regime and kth replication, μ the general mean, g_i the effect of the ith genotype, t_j the effect of the jth Fe regime, $g_i * t_j$ the interaction effect of the ith genotype and the jth Fe regime, r_k the effect of the kth replication, and e_{ijk} the residual error. To estimate adjusted entry means (AEM) for all genotypes, g_i and t_j were considered as fixed and all other effects as random. Furthermore, all effects, except t_j, were considered as random to estimate the genotypic variance (σ^2_g), the interaction variance between genotypes and Fe regime (σ^2_{g*t}), and the error variance (σ^2_e). Statistical significance of σ^2_g and σ^2_{g*t} has been assessed according to Scheipl, Greven, and Küchenhoff (2008). The broad sense heritability H^2 across both Fe regimes was calculated as:

$$H^2 = \frac{\sigma^2_g}{\sigma^2_g + \frac{\sigma^2_{g*t}}{T} + \frac{\sigma^2_e}{T*R}}.$$

In addition, the concentrations of mineral elements collected from each Fe regime were analysed separately using the following mixed model:

$$y_{ik} = \mu + g_i + r_k + e_{ik},$$

where y_{ik} was the observed elemental concentration of the ith genotype in the pot of the kth replication and e_{ik} the residual error. To estimate AEM for all genotypes, g_i was considered as fixed and r_k as random. Furthermore, g_i and r_k were considered as random to estimate σ^2_g and σ^2_e. The broad sense heritability H^2 for each Fe regime was calculated in analogy to the method described above:

$$H^2 = \frac{\sigma^2_g}{\sigma^2_g + \frac{\sigma^2_g}{R}}.$$

Student's t test was used to examine the statistical significance of the mean difference between deficient and sufficient Fe regimes. Pairwise Pearson's correlation coefficients were assessed between the 12 mineral elements examined in the current study, 11 morphological and physiological traits evaluated by Benke et al. (2014), and nine mineral elements measured in maize grains by Baxter et al. (2013). The difference between pairs of correlations was tested using a t-test of the Z-transformed correlations. A principal component (PC) analysis of the normalized and scaled concentrations of 12 mineral elements in the shoot of the maize IBM population as well as the two parental inbred lines measured in sufficient and deficient iron regimes was performed.

All above described statistical analyses were not only performed for the concentration of mineral elements but also for the total content accumulated in the shoots, that is, average content per plant. The average content per plant, which was in the following designated as content was calculated from the product of concentration and the shoot dry weight per plant described by Benke et al. (2014).

2.4 | Ionomic and genomic prediction

The prediction of the presence of an environmental perturbation from the physiological response was performed by applying a logistic regression model with the Fe regime as dependent variable. Two sets of mineral elements were used as independent variables: (a) all mineral elements except Fe and (b) all mineral elements except Fe and Zn. We applied fivefold cross-validation (CV) for validation of these predictions (Hjorth, 1994). For this purpose, the 85 RIL were randomly subdivided into five disjoint subsets. The AEM of one subset for each of the two Fe regimes were left out and used as validation set whereas the other four subsets were used as training set. This procedure was replicated 20 times, yielding in total 100 CV runs. For each of the CV runs, the proportion of genotype*environment combinations from the validation set for which the Fe regime was correctly predicted, was estimated. The median of this proportion across all CV runs was designated as predictive ability.

The physiological and morphological traits assessed by Benke et al. (2014) for the same plants in each of the two Fe regimes were predicted by two predictors: (a) the mineral element concentrations and (b) the molecular marker information described in the next paragraph. W is a matrix of feature measurements for the respective predictor. The dimension of W is determined by the number of RIL and m, the number of features in the corresponding predictor (m_{ionome} = 12, $m_{molecularmarkers}$ = 1,212). The columns in W were centred and standardized to unit variance. For each predictor, an additive relationship matrix was calculated as.

$$G = 1/m + WW^T,$$

where W^T denotes the transpose of W (VanRaden et al., 2009). The additive relationship matrices were used for genomic best linear

unbiased prediction (GBLUP, Meuwissen, Hayes, & Goddard, 2001). GBLUP method was used as implemented in the R package sommer (Covarrubias-Pazaran, 2016). Fivefold CV was applied, as described above. We calculated the predictive ability [r(y_{pred}, y_{obs})] as the Pearson correlation between the observed AEM and the predicted genotypic values.

2.5 | QTL analyses

The publicly available genotypic data for the RIL as well as the genetic map positions of these markers on the IBM2 map were the basis of our analyses. Markers that showed a highly significant ($p < .001$) distorted segregation were excluded. The remaining 1,212 markers were used for the QTL analyses. QTL analyses to detect genome regions linked to the difference in the concentration and content of mineral elements across the two examined Fe regimes were conducted with Rqtl (Broman, Wu, Sen, & Churchill, 2003). Standard interval mapping using the Haley-Knott regression algorithm (Haley & Knott, 1992) and a model that included the Fe regime as additive covariate were used in a first step.

Forward selection was used in the following to determine the maximum number of QTL to include in the model selection procedure. An automated forward and backward search algorithm was then applied to perform multiple QTL mapping using a model that included again the Fe regime as additive covariate. Model selection was based on the highest penalized LOD score with penalties determined through 1,000 permutations. In the next step, the presence of epistatic interaction among all pairs of QTL with main effects were examined. Afterwards, a forward and backward search algorithm was applied to add significant QTL*Fe regime interactions to the model, where significance of all models tested was empirically determined using 1,000 permutations.

Confidence intervals for QTL were calculated using a 1.5 LOD drop technique (Manichaikul, Dupuis, Sen, & Broman, 2006). In order to obtain unbiased estimates of the proportion of the explained phenotypic variance, fivefold CV accounting for genotypic sampling as applied as described earlier for QTL mapping (Utz, Melchinger, & Schön, 2000) and the mean proportion of the phenotypic variance explained by one or multiple QTL (R_{CV}) was calculated.

2.6 | Characterization of genes in QTL confidence intervals

The molecular markers flanking the QTL confidence interval were identified and their physical position on the B73 AGPv4 sequence was derived. For those flanking markers for which a physical map position could not be derived, it was estimated based on the nearest locus on the IBM2 2008 Neighbours map for which a physical positioning was available. The genes in the physical QTL confidence interval were extracted from the B73 AGPv4 sequence. The polymorphisms within the physical confidence interval were extracted from the maize

haplotype version 3 (Bukowski et al., 2018) after converting the assembly to AGPv4 using CrossMap (Zhao et al., 2014). The annotation of these polymorphisms was performed using the Ensembl Variant Effect Predictor (McLaren et al., 2016). Furthermore, selected polymorphisms that are predicted to have a high variant consequence were validated by Sanger sequencing.

After converting the AGPv4 based positions of candidate genes to AGPv2 based, the v2.7 data from genotyping by sequencing experiments of maize inbreds of the USA national seed bank (Romay et al., 2013) was used to extract existing haplotypes based on polymorphism information from the candidate genes. These 1,749 inbreds were considered in our study for which the information of the US state of origin was available in the Germplasm Resources Information Network database. For haplotypes occurring in the entire sample with a frequency >2.5%, a haplotype network was built using an infinite site model (Hamming, 1950).

If not stated differently, all statistical analyses were performed using statistical software R (R Development Core Team, 2016).

3 | RESULTS

We characterized the variability of the shoot concentrations of mineral elements across two Fe regimes using mixed model analyses to quantify the influence of the various sources of variance. For the concentrations of all mineral elements examined in our study, a significant (α = 0.05) genotypic variance (σ^2_g) was observed except for K and Zn (Figure 1). Similarly, σ^2_g was significant (α = 0.05) for the content of all mineral elements except for Cu and Mn. The variance of genotype*Fe regime interactions (σ^2_{g*t}) was on average across the concentrations of all mineral elements even more important than σ^2_g and was significantly different from 0 (α = 0.05) for all mineral elements. In addition, σ^2_{g*t} of the concentrations of mineral elements was considerably more pronounced compared to that of the contents of mineral elements. As a consequence, the broad sense heritabilities (H^2) of the concentrations of mineral elements for the sufficient and deficient Fe regime were with a range from 0.39 to 0.95 slightly higher than H^2 across both Fe regimes, whereas the opposite trend was observed for the mineral element contents.

The AEM for all mineral element concentrations except Fe was on average across all RIL significantly higher (α = 0.05) under the deficient Fe regime compared to the sufficient regime, while the opposite was true for Fe (Figure 2). In contrast, the AEM for the content of all mineral elements except Cd, Cu, Mn, and Zn was on average across all RIL significantly higher (α = 0.05) under the sufficient Fe regime compared to the deficient regime, while the opposite was true for Zn. A strong transgressive segregation was observed in the RIL for the concentrations of all mineral elements which suggests that both parental inbreds contribute alleles to the progenies that increase the concentrations of the studied mineral elements. For the mineral element contents, transgressive segregation was less pronounced compared to that observed for the concentrations of mineral elements.
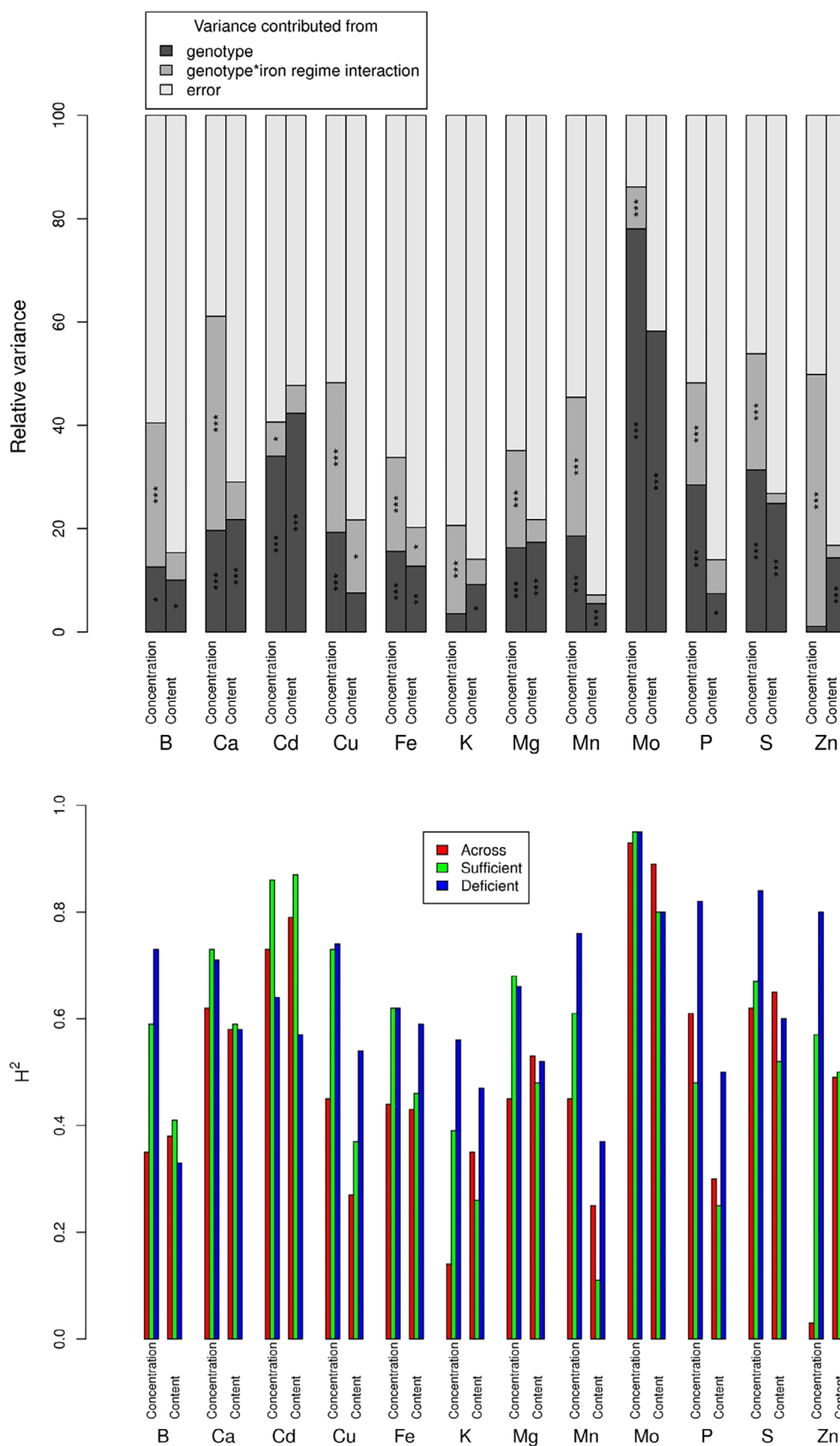
FIGURE 1 Analysis of variance for shoot concentrations and contents of 12 mineral elements. Linear mixed models were used to describe (a) the variance contributed from genotype (σ^2_g), genotype*iron (Fe) regime interaction (σ^2_{g*t}), and error (σ^2_e). σ^2_g and σ^2_{g*t} estimates marked by *, **, and *** are significantly (α = 0.05, 0.01, and 0.001) different from 0. (b) Estimates for heritability (H^2) across as well as for the individual Fe regimes were calculated
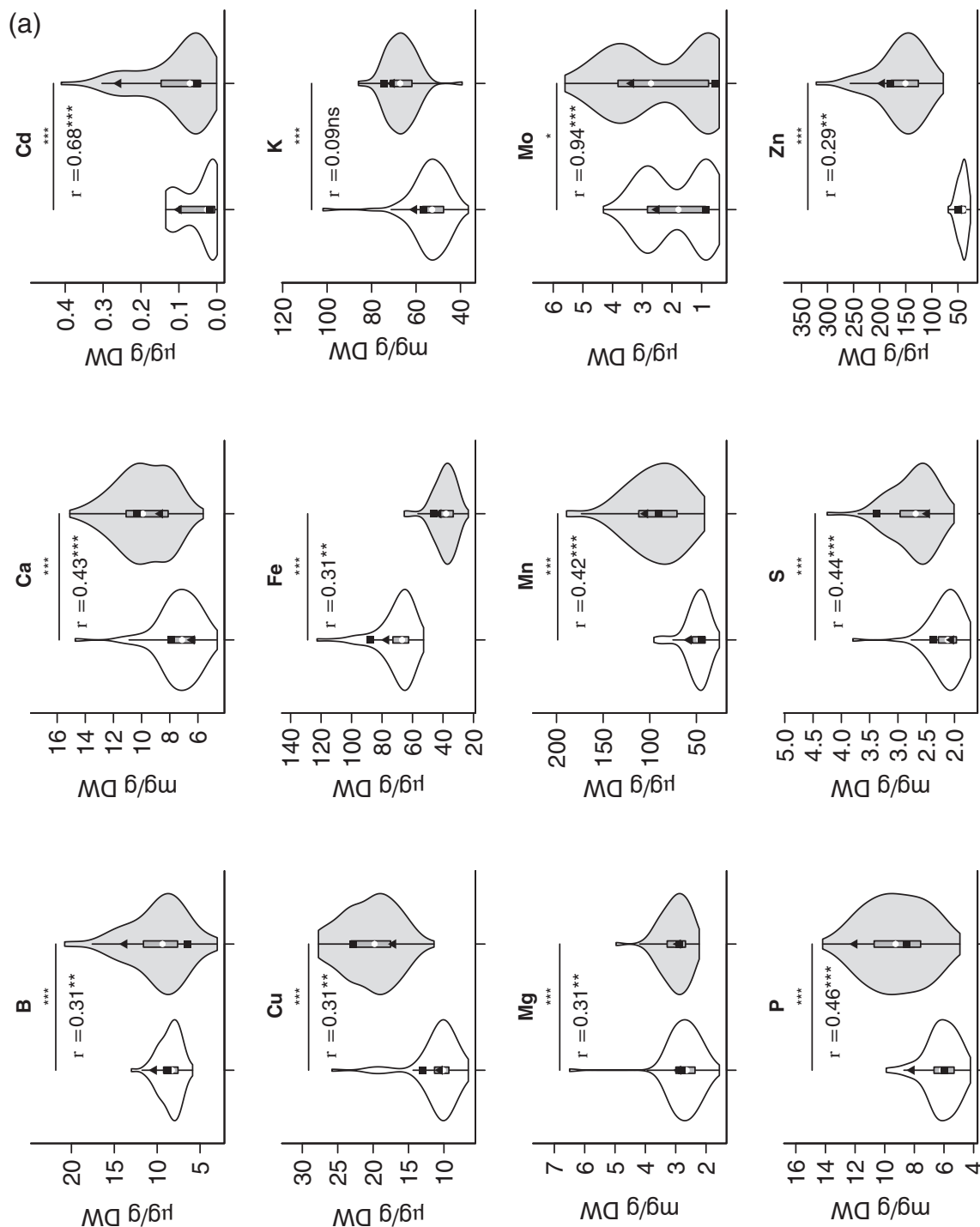
FIGURE 2 Frequency distribution of the adjusted entry means (AEM) of the (a) concentrations, (b) shoot contents of 12 mineral elements in the maize IBM population measured at sufficient (white) and deficient (grey) iron regimes. The AEM of the parental inbreds B73 and Mo17 are represented by a square and a triangle, respectively. The significance level of a *t*-test examining the difference of one mineral element examined in two different iron (Fe) regimes across the population are given above the horizontal line. Pearson's correlation coefficient (ρ) was calculated between the AEM of both Fe regimes. *, **, ***: p = .05, .01, and .001, respectively; ns, not significant

In the PC analysis of the concentrations of mineral elements, the first two principal components explained 19.2 and 13.9% of the variance (Figure S1), where no obvious clustering of the RIL was observed with respect to these two principal components. The same trend was observed in the PC analysis of the mineral element contents (data not shown). The heat map of Pearson's pairwise correlation coefficients between all pairs of mineral elements (Figure 3) revealed that with the exception of Mo and Cd all mineral elements showed higher correlation coefficients within the same Fe regime than the same mineral elements measured in samples from different Fe regimes (Figure S2)
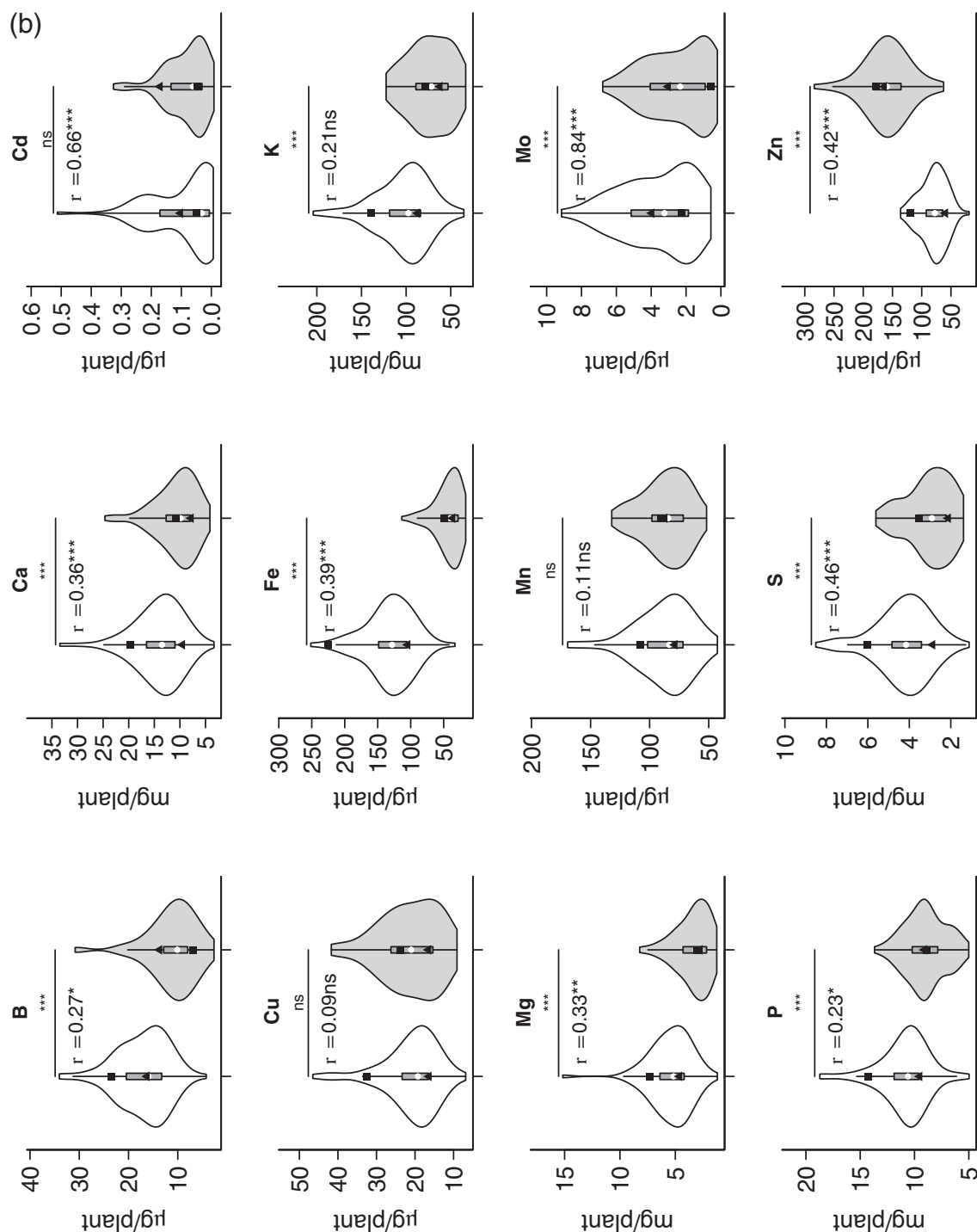
FIGURE 2 (Continued)

regardless of whether the concentration or the content of mineral elements was considered.

The pair of mineral element concentrations with the highest correlation coefficient that was consistent across both Fe regimes was P/Mn, while that with the lowest was Mo/Fe. In total, we observed for 10 pairwise correlations of mineral element concentrations that did not involve Fe significant (α = 0.05) differences between the Fe sufficient and the Fe deficient regime (Figure 4a).

Interestingly, correlations typically found in shoots, such as between Ca and Mg, were strong in the Fe sufficient regime but got lost under Fe deficiency. Other correlations, especially between Zn and Mn became more pronounced under Fe deficiency. The mineral elements that were most frequently involved in the correlations that differed significantly between the Fe sufficient and deficient regime were Ca (four times), Cu, and K (three times), and S, Mg, Mn, P (two times).

(a)

(b)
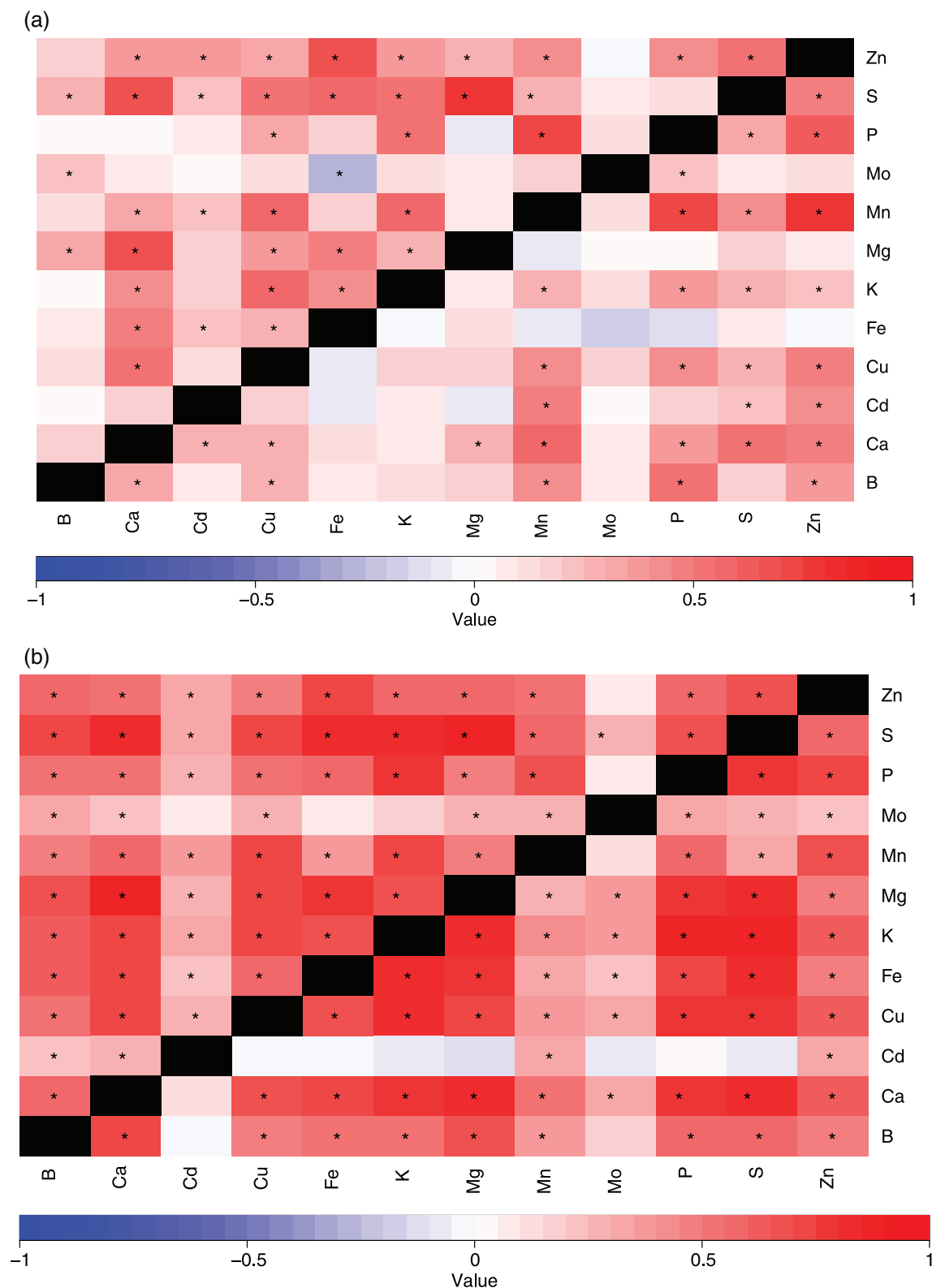
FIGURE 3 Heat map of Pearson's correlation coefficients calculated for all pairs of mineral element (a) concentrations and (b) contents measured in the shoots of the maize IBM population grown under sufficient (above diagonal) and deficient (below diagonal) iron regimes. The cells marked with an asterisk * indicate that the corresponding correlation coefficient was significantly ($\alpha = 0.05$) different from 0 [Colour figure can be viewed at wileyonlinelibrary.com]

The same general trends that were observed for the concentrations of mineral elements were also observed for the contents of mineral elements (Figure 3b). However, the relationship between the

correlation coefficients calculated between the contents of two mineral elements under the Fe sufficient and the Fe deficient regime was more tight than that observed for the concentrations of mineral
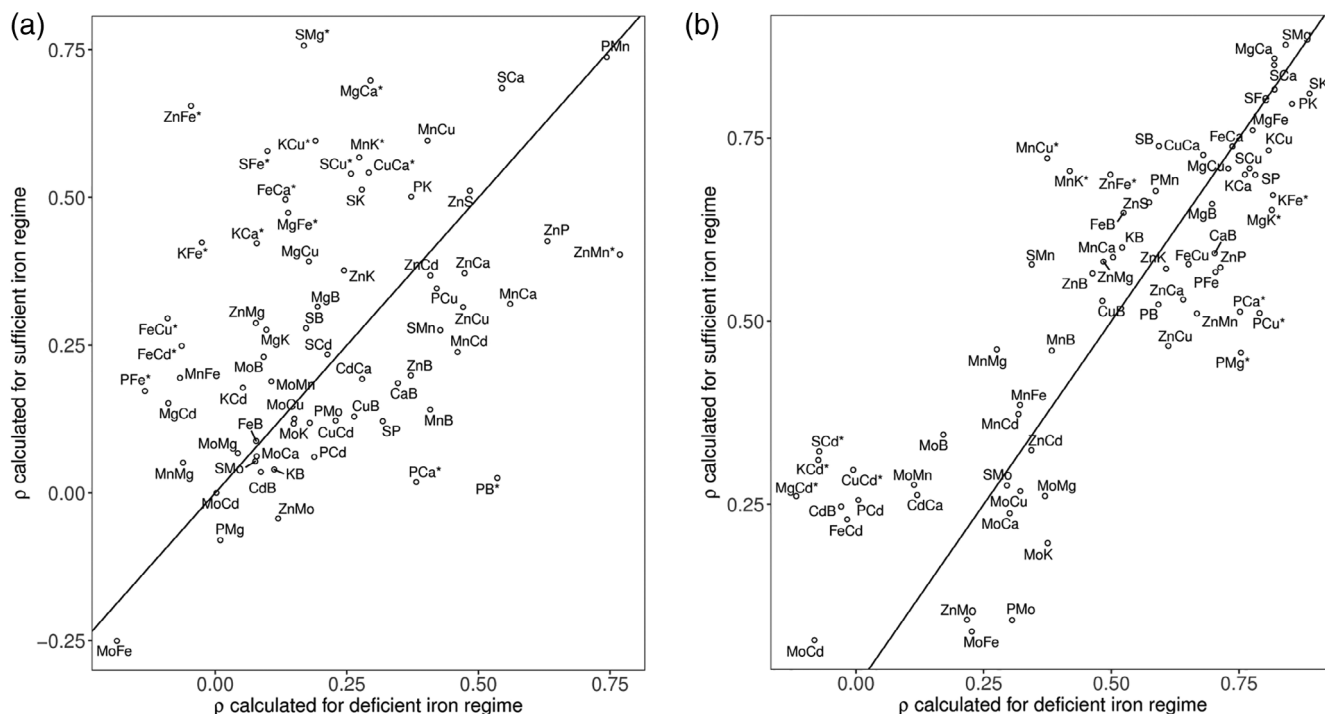
FIGURE 4 Scatterplot of Pearson's correlation coefficient between 12 mineral element (a) concentrations and (b) contents determined in maize shoots harvested from an iron sufficient versus deficient regime. The pairs of correlations that are significantly (α = 0.05) different from each other are markerd by an asterisk *. The linear trendline corresponds to the bisectrix

elements. Nevertheless, also for the contents of mineral elements 10 pairwise correlations not involving Fe differed significantly between the Fe sufficient and deficient regime (Figure 4b). The mineral elements that were most frequently involved in these correlations were P, Cd, K, and Mg (three times), as well as Mo and Mn (two times).

We examined the correlations between the mineral element concentrations in maize shoots and morphological and physiological traits of the same plants (Benke et al., 2014). In the sufficient Fe regime, we observed tight correlations between the shoot concentration of P and root weight (RW), shoot dry weight (SDW), and lateral root formation (LAT), whereas under deficient Fe conditions, the tightest correlations were observed between P, Mn, and Zn concentrations and the shoot dry weight and different leaf greenness parameters (SP) (Figure S3). These correlations were in close agreement with earlier studies and confirmed here across a RIL population.

From the ionomic profile of maize shoots, we evaluated the possibility to predict an environmental perturbation. This was done by predicting the Fe regime in which the RIL of the IBM population was cultivated based on the measured concentrations of mineral elements. When using all mineral elements except Fe and Zn as independent variables, the cross-validated predictive ability was very high with a value of 0.90. This ability increased to 1.0, when Zn was included as independent variable. In a second approach, we examined here the prediction of physiological and morphological traits assessed previously by Benke et al. (2014) in the IBM population from molecular marker data. The cross-validated predictive ability ranged from 0.13

to 0.53 for the sufficient Fe regime (Table 1). For the deficient Fe regime, the observed predictive abilities were higher and ranged from 0.23 to 0.57. The same trend was observed when using the mineral elements as predictors. However, the such observed predictive abilities were for the sufficient Fe regime for five physiological and morphological traits significantly (α = 0.05) higher than for predictions made from molecular marker data. For the deficient Fe regime, this trend was observed for nine of the 11 examined traits.

To unravel the genetic determinants of the shoot ionome of maize, a linkage mapping approach was used. For the concentration of all mineral elements except K, genome regions with significant effects were identified (Table S1). The cross validated proportion of phenotypic variance explained by the genome regions with significant main effect ranged from 0.9 to 66.6%. Seven of the detected 27 genome regions showed a significant interaction with the Fe regime, while for two of the seven genome regions no significant main effect was observed. For none of the QTL with a significant main effect, significant epistatic interactions were observed. The LOD score (up to 5.9) as well as the proportion of the phenotypic variance (up to 2.6%) explained by the QTL*Fe regime interactions were considerably lower than that of the main effect QTL. For the contents of all mineral elements except P, the same trends were observed for the 33 genome regions (Table S2). A total of four genome regions that contributed significantly to the phenotypic variance of the concentration of mineral elements (C-Cd1, C-Cu2, C-Mo1, C-Mo5) contributed also to the content of the same mineral element (A-Cd1, A-Cu3, A-Mo1, A-Mo4). In general, we observed a clustering of genome regions that

TABLE 1 Median and standard deviation of predictive ability [$r(y_{pred}, y_{obs})$] of ionomic/genomic prediction in the IBM population for physiological and morphological traits (Benke et al., 2014) obtained across 100 fivefold cross-validation runs with the prediction method genomic best linear unbiased prediction

Trait	Sufficient			Deficient		
	Mineral element concentrations	Molecular markers	Difference	Mineral element concentrations	Molecular markers	Difference
SP3	0.31 ± 0.18	0.36 ± 0.18	Ns	0.61 ± 0.13	0.40 ± 0.18	*
SP4	0.57 ± 0.14	0.25 ± 0.20	*	0.69 ± 0.12	0.50 ± 0.17	*
SP5	0.39 ± 0.19	0.48 ± 0.17	*	0.74 ± 0.10	0.38 ± 0.16	*
SP6	0.35 ± 0.19	0.50 ± 0.18	*	0.76 ± 0.09	0.37 ± 0.18	*
RL	0.05 ± 0.21	0.13 ± 0.24	*	0.45 ± 0.16	0.24 ± 0.25	*
RW	0.56 ± 0.19	0.28 ± 0.21	*	0.68 ± 0.18	0.37 ± 0.20	*
SL	0.41 ± 0.19	0.26 ± 0.16	*	0.59 ± 0.15	0.36 ± 0.18	*
SDW	0.62 ± 0.16	0.31 ± 0.20	*	0.77 ± 0.10	0.31 ± 0.21	*
WC	0.37 ± 0.21	0.53 ± 0.17	*	0.36 ± 0.19	0.57 ± 0.17	*
LAT	0.65 ± 0.15	0.17 ± 0.22	*	0.60 ± 0.17	0.31 ± 0.17	*
NEC	0.23 ± 0.20	0.19 ± 0.22	Ns	0.22 ± 0.21	0.23 ± 0.18	Ns

Note: The considered traits were the relative chlorophyll content of leaf 3–6 (SP3, SP4, SP5, and SP6), root length (RL), root weight (RW), shoot length (SL), shoot dry weight (SDW), water content (H_2O), lateral root formation (LAT), and leaf necrosis rating (NEC).

contribute significantly to the phenotypic variance on chromosomes 1, 5 and 7 (Figure 5). Nevertheless, the high mapping resolution of the IBM population allowed for all except four pairs of QTL for the concentration of mineral elements a separation of the effects. For the mineral element contents, the number of overlapping pairs of QTL was with 10 considerably higher. The two most prominent QTL explaining in CV at least 39% of the phenotypic variance and that were detected for the concentration as well as the content of mineral elements were *C-Cd1/A-Cd1* as well as *C-Mo1/A-Mo1* (Figure 6). At all of these four QTL, the Mo17 allele increased the concentration or content of the corresponding mineral element.

Two genes (Zm00001d005189 and Zm00001d005190) were located within the confidence interval of *C-Cd1/A-Cd1* that both have an annotation as cadmium/zinc-transporting ATPase. The gene Zm00001d033053 that was located within the confidence interval of *C-Mo1/A-Mo1* has an annotation as molybdate transporter 1. Because polymorphisms in these genes contribute to phenotypic variation of Cd and Mo in other plant species, we evaluated the polymorphisms in these three genes in detail (Figure 7). Zm00001d005189 has an early stop codon in B73 that is absent in Mo17. For Zm00001d005190 (*C-Cd1/A-Cd1*), Mo17 gained a stop codon compared to B73 at position 163,039,505 where it lost one at position 163,039,743. The SNP observed in the sequence of the genes Zm00001d033053 (*C-Mo1/A-Mo1*) caused a change in a single amino acid. These polymorphisms, which were detected in the maize haplotype version 3, have been validated using Sanger sequencing (data not shown).

We mined the data from genotyping by sequencing experiments of 1,749 maize inbreds of the USA national seed bank and explored the existing haplotypes at the three genes as well as their frequency. For Zm00001d033053 only a reduced set of polymorphisms that did not allow any differentiation between B73 and Mo17 haplotypes was

found. For Zm00001d005189 and Zm00001d005190, B73 haplotypes occurred with high frequency in the studied set of maize inbreds (Supplementary Figure 4), whereas the Mo17 allele was underrepresented compared to genome-wide data. In addition, no obvious clustering of the haplotypes with respect to the state of origin of the respective inbred was observed (data not shown).

4 | DISCUSSION

4.1 | Natural variation in the mineral element profile of maize shoots and the interaction with the Fe regime

Across the RIL of the IBM population, we observed a high phenotypic variability in the concentration but also the content of all mineral elements (Figure 2). The performed mixed-model analyses revealed that for most mineral elements concentrations as well as contents this variation was due to significant (α = 0.05) genotypic (σ^2_g) variance (Figure 1). These findings indicate that the examined population is appropriate to be used to identify the genetic factors that contribute to the variation of mineral element concentrations in maize shoots. This holds especially true as we have studied an intermated RIL population, in which additional rounds of intermating cause a rapid decay of linkage disequilibrium. Thus, correlations between mineral elements observed in our study are less likely caused by linkage but are rather due to pleiotropy. Therefore, the examined population is also particularly suitable to validate correlations among mineral elements.

The correlations between pairs of concentrations of mineral elements that were observed in our study under the Fe sufficient regime (Figure 3) were generally in good agreement with those observed in
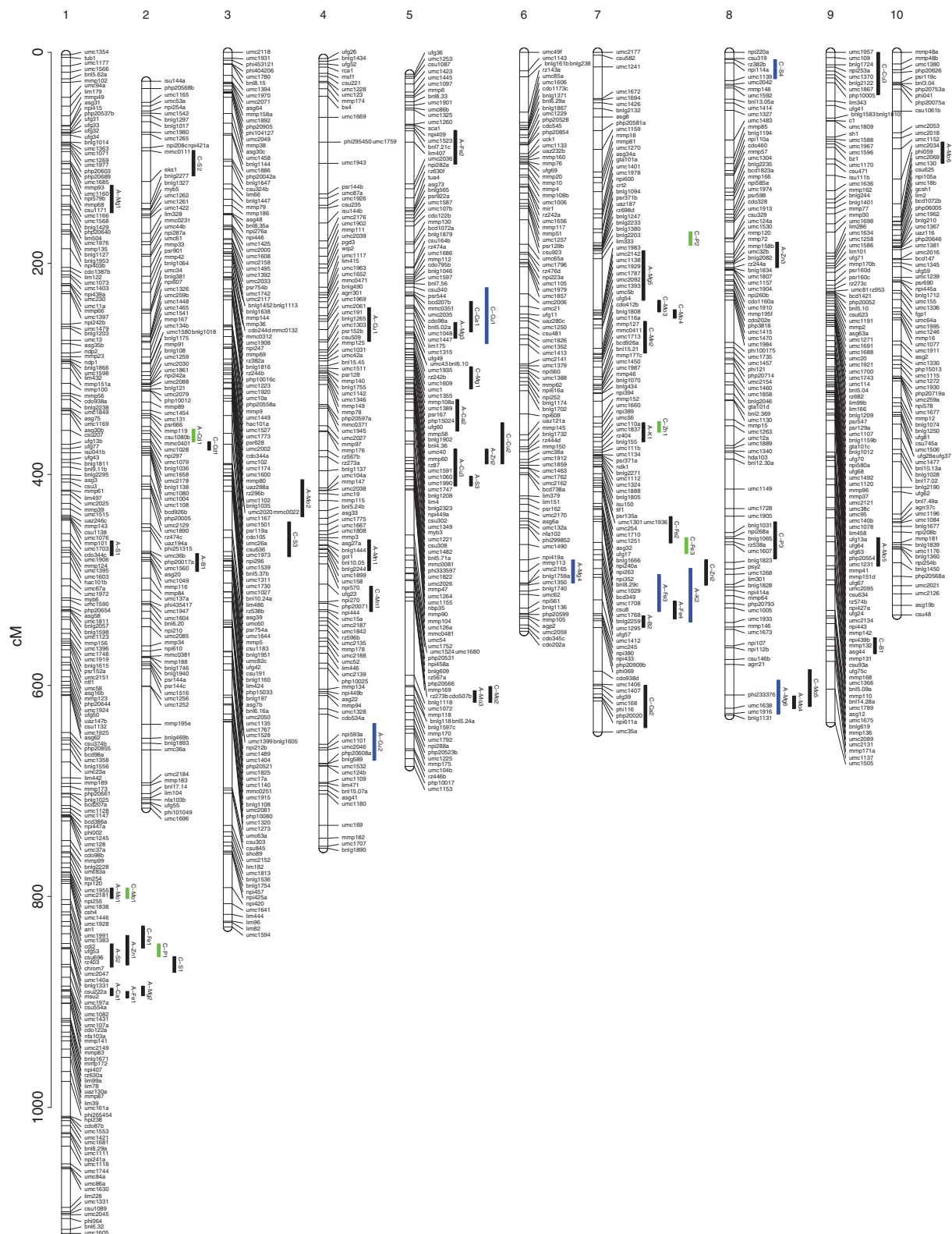
FIGURE 5 Confidence intervals of the detected quantitative trait loci (QTL) for shoot concentrations (C-*) and contents (A-*) of 12 mineral elements on the IBM2 map of maize. QTL, for which the interval is coloured in black, showed only significant main effects. Green and blue QTL confidence intervals indicate QTL with significant main and interaction effects as well as QTL with only significant interaction effects, respectively [Colour figure can be viewed at wileyonlinelibrary.com]
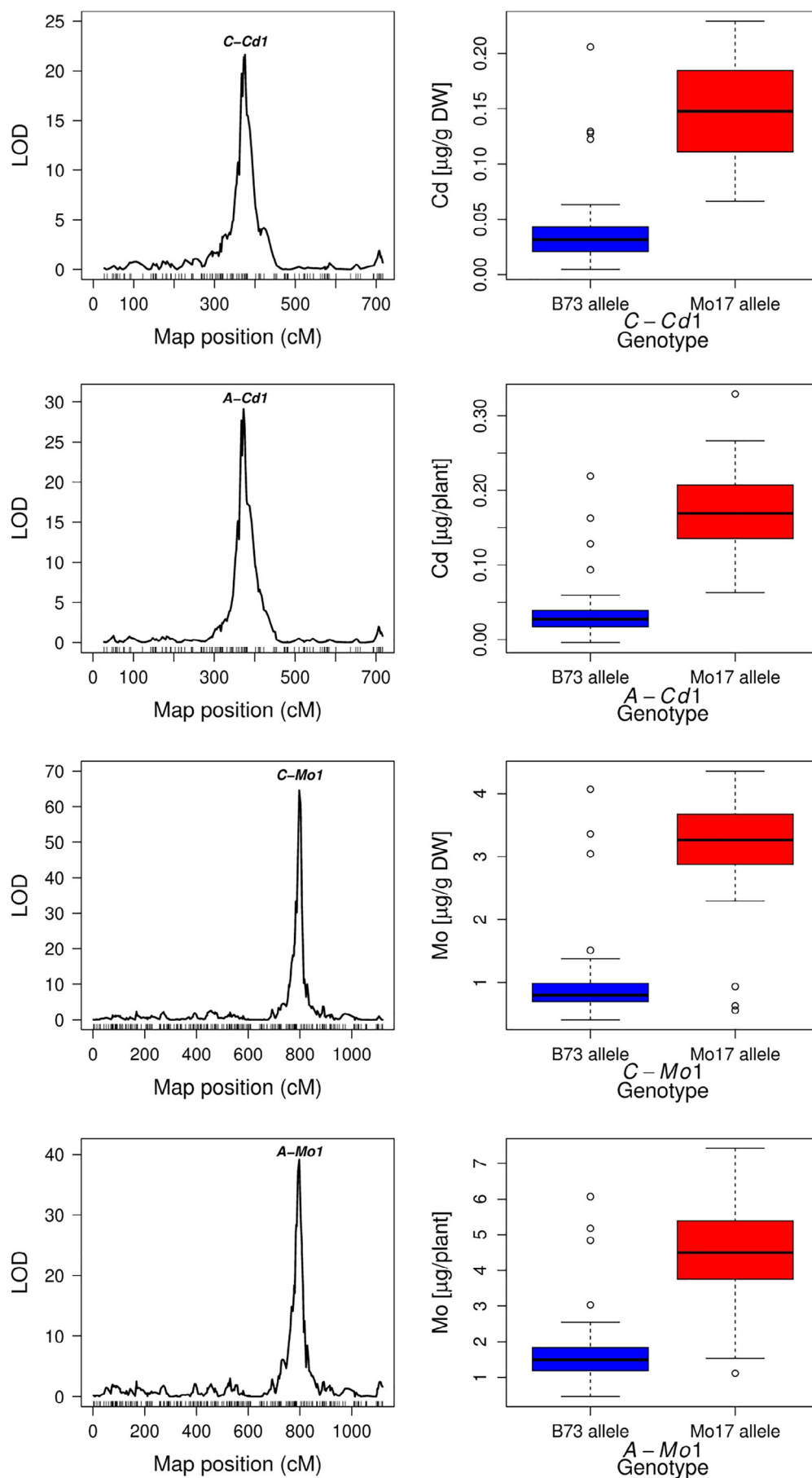
FIGURE 6 The plots in the left column present the logarithm of odds (LOD) versus the position on the genetic map of chromosomes two, two, one, and one, respectively, for a selected set of quantitative trait loci (QTL) with significant main effects across two iron regimes for cadmium (Cd) and molybdenum (Mo) concentration (C-*) and content (A-*) in shoots of the maize IBM population. The plots in the right column are boxplots of the adjusted entry means of the genotypes carrying the B73 or Mo17 allele at the QTL position across the sufficient and deficient Fe regime [Colour figure can be viewed at wileyonlinelibrary.com]
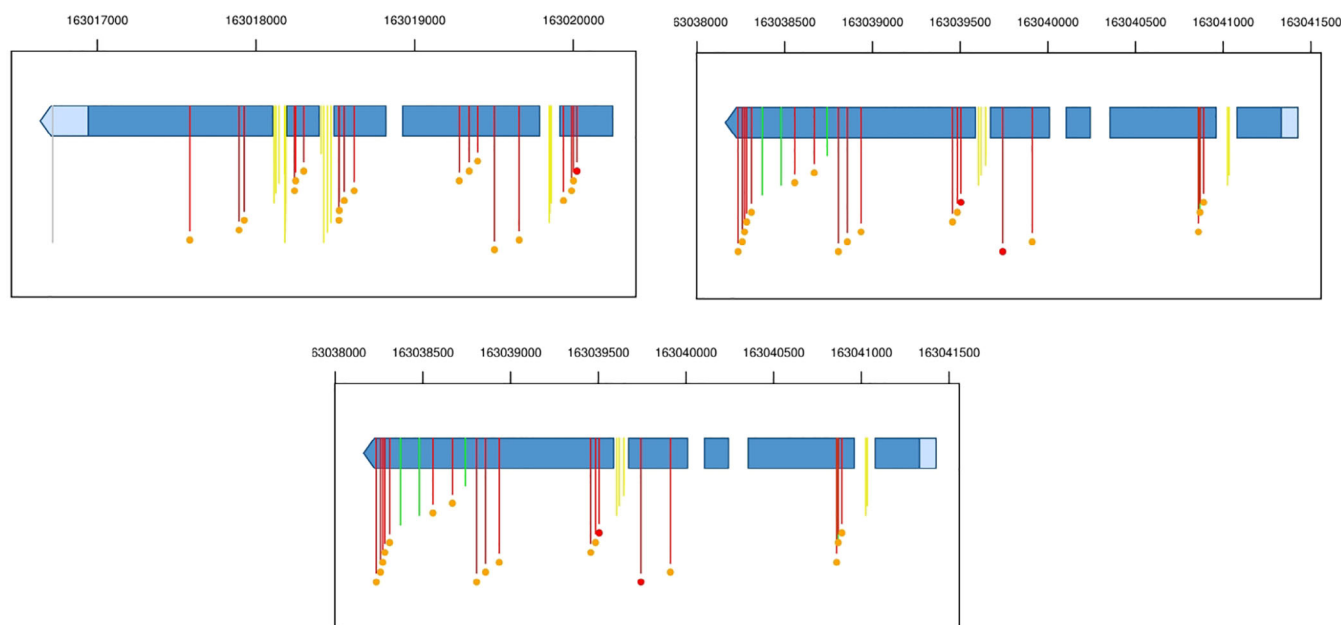
FIGURE 7 Schematic gene model of the first transcript of candidate genes for *C-Cd1/ACd1* (first row) and *C-Mo1/A-Mo1* (second row). Blue boxes indicate exons. Light blue boxes indicate untranslated regions (UTRs). Vertical lines indicate polymorphisms between B73 and Mo17, where grey is used for polymorphisms in 3′ and 5′ UTR, yellow for intron variants, green for synonymous, and red for non-synonymous polymorphisms in the coding sequence, respectively. The orange or red disk below the polymorphisms indicates a moderate or high severity of the variant consequence, respectively. The y-axes indicate the positions of the polymorphisms in bp on the corresponding chromosomes [Colour figure can be viewed at wileyonlinelibrary.com]

earlier studies with maize (Baxter et al., 2013) but also with *Brassica napus* (Bus et al., 2014) or with 334 angiosperm species (Neugebauer, Broadley, El-serehy, & George, 2018). In contrast to previous studies, we not only assessed the concentration of mineral elements but also the shoot content. Shoot contents reflect the cumulative uptake and translocation of mineral elements to the above-ground biomass of a plant over the whole growth period. The proportion of pairs of mineral element concentrations with a significant positive correlation (Figures 3 and 4) was much lower than that for the contents of mineral elements and this finding was independent of the considered Fe regime. This observation is explained by the variation in biomass which was in the Fe sufficient regime >threefold and even higher in the Fe-deficient regime (Benke et al., 2014). Thus, shoot contents correct for differences in biomass, which were here mostly related to the genotype rather than the genotype*environment interaction. In our RIL, the latter made only a minor contribution to the overall variance in element concentrations and even less in shoot element contents (Figure 1a).

Due to the design of our study that is, the assessment of the shoot ionome of the IBM population in two contrasting Fe regimes, we were not only able to validate correlations between pairs of mineral elements but to compare the correlation of two mineral elements across different Fe regimes. By that, we identified interactions among Fe and two other mineral elements. We observed significant (α = 0.05) differences in 10 pairwise correlations of mineral element concentrations between the Fe sufficient and deficient regime that did not involve Fe (Figure 4a).

Maybe most prominent is the positive interaction between Ca and Mg, which in angiosperms has been related to cation exchange

capacities in the cell wall of leaves (White, Broadley, El-Serehy, George, & Neugebauer, 2018). This and other correlations got lost under Fe deficiency, when more negative correlations prevailed (Figure 4a). A major determinant for this shift is the degradation of suberin in the root endodermis under Fe deficiency, which in Arabidopsis has been shown to form an apoplastic barrier that is regulated by the nutritional status of the plant (Barberon et al., 2016). The degradation increases the endodermal passage and subsequent root-to-shoot translocation particularly of Ca, Mn and Zn (Baxter et al., 2009). Hence, correlations between these and other elements disappear under Fe deficiency, while new ones are formed between elements that profit in the same way, as Zn and Mn (Figure 4a).

Earlier studies have reported the interaction of Fe with the concentration of several mineral elements, mostly with S, P or other metals (Astolfi, Zuchi, Passera, & Cesco, 2003; Kanai, Hirai, Yoshiba, Tadano, & Higuchi, 2009; Mori & Nishizawa, 1987; Zheng et al., 2009). Under Fe deficiency, all of these correlations turned more negative (Figure 4a), which is not only related to endodermal suberization but also to the Fe deficiency-induced expression of genes involved in Fe acquisition which favour also Zn and Mn acquisition (Eroglu, Meier, Wiren, & Peiter, 2016; Leskova, Giehl, Hartmann, Fargasova, & von Wiren, 2017). In maize, this includes the release of phytosiderophores and uptake of phytosiderophore-chelated metals, such as Zn, Cu and Ni (Schaaf et al., 2004; von Wiren et al., 1996).

In addition, we observed a particularly strong difference between the correlations of P and all mineral elements except Fe and B assessed in the two Fe regimes. In the sufficient Fe regime, all these correlations were positive while in the deficient Fe regime these

correlations were negative (Figure 4a). This link between P and Fe is in accordance with earlier studies. DeKock, Hall, and Inkson (1979) and Zheng et al. (2009) have shown that elevated P supplies decrease the availability and mobility of Fe in soils as well as in plants and therewith provoke Fe deficiency-induced chlorosis (Ajakaiye, 1979). The results of Shi et al. (2018) indicate that Fe retention in the hemicellulose fraction of roots is an important determinant of the tolerance to Fe deficiency-induced chlorosis of graminaceous plant species with low phytosiderophore release, like maize. Then, P-dependent Fe retention in the hemicellulose fraction may become a determining factor for Fe provision of the shoot and, thus, for chlorosis susceptibility.

With the increasing knowledge on such mechanistic processes underlying nutrient correlations, the shoot ionome becomes more and more informative (Huang & Salt, 2016) and paves the way to identify and assign anatomical changes or physiological processes to allelic variation.

4.2 | Predictive power of the shoot ionome

Baxter et al. (2008) showed that the impact of an environmental perturbation on a plant can be predicted by changes in its ionome. While this principle was demonstrated for the Col-0 accession in *A. thaliana* when subjected to Fe deficiency, we first addressed the question whether the shoot ionome is also a reliable predictor for the nutritional status in a RIL population subjected to the same nutritional perturbation. Using the IBM population for this purpose is especially meaningful, because it has been generated from a cross between two parental lines opposing in P and Fe efficiency (Benke et al., 2014; Kaeppler et al., 2000; Shi et al., 2018). Indeed, our analysis revealed a cross-validated predictive ability of 0.90 when predicting the Fe-regime, in which the RIL of the IBM population were cultivated. This was based on the measured concentrations of mineral elements, except for Fe and Zn. Predictive ability increased to 1.0 when including Zn. Likewise, a study with 19 different Arabidopsis accessions showed that changes in the shoot ionome can be employed to distinguish accessions according to their Zn nutritional status (Campos et al., 2017). These findings indicate that even across diverse genetic materials, the profile of the mineral elements is a reliable proxy for the physiological state and allows identifying nutritional perturbations.

We then addressed the question whether the shoot ionome is also a reliable predictor for morphological and physiological traits perturbed by an altered Fe regime. In fact, when predicting from the concentration of mineral elements, physiological and morphological traits of individual RIL (cf. Benke et al., 2014), cross-validated predictive abilities up to 0.77 were observed (Table 1). An increasing prediction ability under Fe deficiency indicated that an imposed nutritional disorder even increases the predictive power of the ionome.

We then compared the prediction of physiological and morphological traits by mineral elements with that by molecular markers. Unexpectedly, ionome-based predictive abilities were considerably higher compared to the predictive abilities based on molecular marker profiles using GBLUP (Table 1). A likely explanation is that the variation of mineral element concentrations are in direct functional relationship to the physiological and morphological traits examined in the frame of our study. This is emphasized by the observation that molecular marker-based prediction values responded less to Fe deficiency. We thus conclude that mineral element profiles are powerful predictors of physiological and morphological traits. Their use for the prediction of further, for example, yield-related traits, should be examined in further studies.

4.3 | Genetics of the shoot ionome

In contrast to most previous studies examining the inheritance of the ionome of different species in single environments or in multiple environments that differ with respect to multiple environmental factors (e.g. Asaro et al., 2016; Bus et al., 2014; Shakoor et al., 2016), we analysed the inheritance under two different environmental conditions that differed only with respect to one environmental factor, in our case the Fe regime. This allows to separate the genotype*Fe regime interaction from the genotype*environment interaction, where the former is biologically easier to interpret.

In this study, we exploited the significant genotypic and genotype*Fe regime interaction variance found in the IBM population (Figure 1a) and employed quantitative genetic analyses in order to dissect this variation in the underlying genetic factors. For all mineral elements examined in the frame of this study, except for the concentration of K and the content of P, genomic regions were identified that explained a significant part of the genotypic or genotype*Fe regime interactions (Table S1 and S2). The proportion of variance explained for one mineral element by all QTL interacting with the environment simultaneously was considerably lower than that of the main effect QTL. This finding suggests that albeit the variance of genotype*Fe regime interactions for the concentration of mineral elements was considerably higher than the genotypic variance (Figure 1) the QTL interacting with the environment were not detected in our study. One major reason might be that each QTL explains only a small proportion of the genotype*Fe interaction.

Due to the use of the IBM population, which has compared to non intermated linkage mapping populations an increased mapping resolution (Lee et al., 2002), the confidence intervals observed in our study were small for most of the 60 QTL (Table S1 and S2). Out of the detected QTL, four QTL had overlapping confidence intervals for the concentrations and contents of the same mineral element. Two of these pairs of QTL jutted out regarding the LOD score as well the proportion of the explained phenotypic variance and these will be discussed in more detail.

4.3.1 | C-Cd1 and A-Cd1

We did not add Cd to the nutrient solution in which the IBM population was cultivated. Nevertheless, we observed under both Fe regimes low Cd concentrations in maize shoots. To rule out the effect of Cd

translocation from the seeds to the growing shoot tissue, we evaluated the Cd concentrations in the grains of a subset of the IBM population. The overall amount of Cd in the grain made up less than 4% of the shoot content, that is, the total amount of Cd accumulated in the above-ground biomass. This indicated that the highly heritable pattern of Cd concentrations that we observed (Figure 1) was caused by Cd traces in the chemicals or the technical devices used to prepare the nutrient solution. As therefore all RIL were exposed systematically to the same Cd concentration in the nutrient solution, we interpreted the observed variation in our study.

We detected in our study two overlapping QTL on chromosome 2 for Cd concentration and content. These QTL were in very good accordance with the QTL detected for Cd content in maize kernels observed in a B73*IL13H population by Baxter et al. (2014). This observation indicates that the mechanisms contributing to the accumulation and sequestration of this mineral element in maize shoots and kernels are similar. However, for nine other mineral elements, correlation coefficients between the mineral element concentrations in maize shoots from our study and in maize kernels from Baxter et al. (2013) were low (data not shown). Hence, a common regulation across tissues exists for some mineral elements but not for all.

Across both Fe regimes, the trait-decreasing allele was provided by B73 (Figure 6). This indicated that inbreds and hybrids carrying the B73 allele are suitable to produce maize on soils with increased Cd accumulations without increasing the Cd concentration in the harvest product.

Within the confidence interval of *C-Cd1/A-Cd1* two genes, Zm00001d005189 and Zm00001d005190, were located directly adjacent to each other that are annotated as *HMA* genes. In the coding sequence of both genes, non-synonymous polymorphisms have been identified that are predicted (McLaren et al., 2016) to have moderate or even high variant consequence (Figure 7). Zm00001d005189 is based on its amino acid sequence not of particular similarity to any of the HMA genes of Arabidopsis or rice (data not shown). In contrast, Zm00001d005190 has a high homology to *OsHMA3* indicating that Zm00001d005190 could be the ortholog *ZmHMA3* which is in accordance with results of Zhao et al. (2018).

Our result indicated that the Mo17 allele at Zm00001d005190, which is presumably non-functional, is present at medium frequency in the maize germplasm of the USDA genebank. This suggests that under regular field conditions the higher accumulation of Cd does not have a negative agronomic side effect. Another explanation is that commercially used maize hybrids are typically crosses between B73-type and Mo17-type inbreds. In this case, the hybrids do not show increased Cd contents, as the functional allele of B73 is expected to be at least partially dominant over the loss-of-function allele of Mo17 (cf. Kuromori, Takahashi, Kondou, Shinozaki, & Matsui, 2009).

4.3.2 | C-Mo1 and A-Mo1

In the confidence interval of these QTL, a homolog of *A. thaliana's* Mo transporter (*MOT1*) (Tomatsu et al., 2007) was detected. We observed

between the coding sequences of B73 and Mo17 one non-synonymous sequence variant (Figure 7) that is predicted to have only a medium effect on the protein. Instead, in accordance with findings of Baxter et al. (2008) for *A. thaliana*, we consider differences in gene expression as more relevant, because in the deficient Fe regime mRNA levels of Zm00001d033053 were about 1,000-fold higher in Mo17 than in B73, whereas in the sufficient Fe regime this difference was only sixfold (Urbany et al., 2013). This Fe dependence of the Mo accumulation was not only observed at the gene expression level but also at the QTL level. *C-Mo1* showed the strongest QTL*Fe regime interaction of this study. However, further research is required to unravel the molecular mechanism of the interaction between Fe and Mo.

5 | CONCLUSIONS

Our results suggest that the shoot ionome is under tight genetic control, and that strong interactions of a genotype with the environment, in our case the Fe regime, are driving the variation for the concentration as well as the content of mineral elements. Furthermore, the high predictive abilities found in this study indicate that mineral elements are powerful predictors of morphological and physiological traits. Their use for the prediction of further, for example, yield-related traits, merits to be examined in further studies. We propose that *ZmHMA2/3* and *ZmMOT1* are major players in the natural genetic variation of Cd and Mo concentrations and contents in maize shoots. Furthermore, our results indicate that even in elite breeding material non-functional alleles segregate at major genes for uptake and translocation of different mineral elements.

CONFLICT OF INTEREST
The authors declare no conflicts of interest.

ORCID
Benjamin Stich https://orcid.org/0000-0001-6791-8068

REFERENCES

Ajakaiye, C. O. (1979). Effect of phosphorous on growth and iron nutrition of millet and sorghum. *Plant and Soil*, *51*, 551–561.

Asaro, A., Ziegler, G., Ziyomo, C., Hoekenga, O. A., Dilkes, B. P., & Baxter, I. (2016). The interaction of genotype and environment determines variation in the maize kernel ionome. *G3*, *6*(12), 4175–4183.

Astolfi, S., Zuchi, S., Passera, C., & Cesco, S. (2003). Does the sulfur assimilation pathway play a role in the response to Fe deficiency in maize (*Zea mays* L.) plants? *Journal of Plant Nutrition*, 26, 2111–2121.

Barberon, M., Bellis, D. D., Takano, J., Salt, D. E., Geldner, N., Barberon, M., ... Naseer, S. (2016). Adaptation of root function by nutrient-induced plasticity of endodermal differentiation. *Cell*, 164(3), 447–459.

Baxter, I., Hermans, C., Lahner, B., Yakubova, E., Tikhonova, M., Verbruggen, N., ... Salt, D. (2012). Biodiversity of mineral nutrient and trace element accumulation in *Arabidopsis thaliana*. *PLoS One*, 7, e35121.

Baxter, I., Hosmani, P. S., Rus, A., Lahner, B., Borevitz, J. O., Mickelbart, M. V., ... Salt, D. E. (2009). Root suberin forms an extracellular barrier that affects water relations and mineral nutrition in Arabidopsis. *PLoS Genetics*, 5, e1000492.

Baxter, I. R., Gustin, J. L., Settles, A. M., & Hoekenga, O. A. (2013). Ionomic characterization of maize kernels in the intermated B73 x Mo17 population. *Crop Science*, 53, 208–220.

Baxter, I. R., Vitek, O., Lahner, B., Muthukumar, B., Borghi, M., Morrissey, J., ... Salt, D. E. (2008). The leaf ionome as a multivariable system to detect a plant's physiological status. *Proceedings of the National Academy of Sciences*, 105(33), 12081–12086.

Baxter, I. R., Ziegler, G., Lahner, B., Mickelbart, M. V., Foley, R., Danku, J., ... Hoekenga, O. A. (2014). Single-kernel ionomic profiles are highly heritable indicators of genetic and environmental influences on elemental accumulation in maize grain (*Zea mays*). *PLoS One*, 9(1), e87628.

Bej, S., & Basak, J. (2014). MicroRNAs: The potential biomarkers in plant stress response. *American Journal of Plant Sciences*, 5, 748–759.

Benke, A., Urbany, C., Marsian, J., Shi, R., Wiren, N. V., & Stich, B. (2014). The genetic basis of natural variation for iron homeostasis in the maize IBM population. *BMC Plant Biology*, 14, 12.

Bentsink, L., Yuan, K., Koornneef, M., & Vreugdenhil, D. (2003). The genetics of phytate and phosphate accumulation in seeds and leaves of *Arabidopsis thaliana*, using natural variation. *Theoretical and Applied Genetics*, 106(7), 1234–1243.

Blair, M. W., Astudillo, C., Grusak, M. A., Graham, R., & Beebe, S. E. (2009). Inheritance of seed iron and zinc concentrations in common bean (*Phaseolus vulgaris* L.). *Molecular Breeding*, 23(2), 197–207.

Broman, K. W., Wu, H., Sen, S., & Churchill, G. A. (2003). R/QTL: QTL mapping in experimental crosses. *Bioinformatics*, 19(7), 889–890.

Bukowski, R., Guo, X., Lu, Y., Zou, C., He, B., Rong, Z., ... Xu, Y. (2018). Construction of the third-generation *Zea mays* haplotype map. *GigaScience*, 7(4), 1–12.

Bus, A., Körber, N., Parkin, I. A. P., Samans, B., Snowdon, R. J., Li, J., & Stich, B. (2014). Species- and genome-wide dissection of the shoot ionome in *Brassica napus* and its relationship to seedling development. *Frontiers in Plant Science*, 5(485), 485.

Campos, A. C. A., Kruijer, W., Alexander, R., Akkers, R. C., Danku, J., Salt, D. E., & Aarts, M. G. (2017). Natural variation in *Arabidopsis thaliana* reveals shoot ionome, biomass, and gene expression changes as biomarkers for zinc deficiency tolerance. *Journal of Experimental Botany*, 68(13), 3643–3656.

Covarrubias-Pazaran, G. (2016). Genome-assisted prediction of quantitative traits using the R package sommer. *PLoS One*, 11(6), 1–15.

DeKock, P., Hall, A., & Inkson, R. (1979). Active iron in plant leaves. *Annals of Botany*, 43(6), 737–740.

Eroglu, S., Meier, B., Wiren, N. V., & Peiter, E. (2016). The vacuolar manganese transporter MTP8 determines tolerance to iron deficiency-induced chlorosis in Arabidopsis. *Plant Physiology*, 170, 1030–1045.

Ghandilyan, A., Barboza, L., Tisne, S., Granier, C., Reymond, M., Koornneef, M., ... Aarts, M. G. M. (2009). Genetic analysis identifies quantitative trait loci controlling rosette mineral concentrations in *Arabidopsis thaliana* under drought. *New Phytologist*, 184(1), 180–192.

Gu, R., Chen, F., Liu, B., Wang, X., Liu, J., Li, P., ... Yuan, L. (2015). Comprehensive phenotypic analysis and quantitative trait locus identification

for grain mineral concentration, content, and yield in maize (*Zea mays* L.). *Theoretical and Applied Genetics*, 128(9), 1777–1789.

Haley, C. S., & Knott, S. A. (1992). A simple regression method for mapping quantitative trait loci in line crosses using flanking markers. *Heredity*, 69(4), 315–324.

Hamming, R. (1950). Error detecting and error correcting codes. *Bell System Technical Journal*, 29, 147–160.

Hjorth, J. (1994). *Computer intensive statistical methods. Validation, model selection and bootstrap*. London, England: Chapman & Hall.

Huang, X. Y., & Salt, D. E. E. (2016). Plant ionomics: From elemental profiling to environmental adaptation. *Molecular Plant*, 9(6), 787–797.

Kaeppler, S. M. S., Parke, J. L., Mueller, S. M., Senior, L., Stuber, C., & Tracy, W. F. (2000). Variation among maize inbred lines and detection of quantitative trait loci for growth at low P and responsiveness to arbuscular mycorrhizal fungi. *Crop Science*, 40, 358–364.

Kanai, M., Hirai, M., Yoshiba, M., Tadano, T., & Higuchi, K. (2009). Iron deficiency causes zinc excess in *Zea mays*. *Soil Science & Plant Nutrition*, 55(2), 271–276.

Klein, M. A., & Grusak, M. A. (2009). Identification of nutrient and physical seed trait QTL in the model legume *Lotus japonicus*. *Genome*, 52, 677–691.

Kuromori, T., Takahashi, S., Kondou, Y., Shinozaki, K., & Matsui, M. (2009). Phenome analysis in plant species using loss-of-function and gain-of-function mutants. *Plant and Cell Physiology*, 50(7), 1215–1231.

Lahner, B., Gong, J., Mahmoudian, M., Smith, E. L., Abid, K. B., Rogers, E. E., ... Salt, D. E. (2003). Genomic scale profiling of nutrient and trace elements in *Arabidopsis thaliana*. *Nature Biotechnology*, 21(10), 1215–1221.

Lee, M., Sharopova, N., Beavis, W. D. G. D., Katt, M., Blaie, D., & Hallauer, A. (2002). Expanding the genetic map of maize with the intermated B73*Mo17 (IBM) population. *Plant Molecular Biology*, 48, 453–461.

Leskova, A., Giehl, R. F., Hartmann, A., Fargasova, A., & von Wiren, N. (2017). Heavy metals induce iron deficiency responses at different hierarchic and regulatory levels. *Plant Physiology*, 174(3), 1648–1668.

Manichaikul, A., Dupuis, J., Sen, S., & Broman, K. W. (2006). Poor performance of bootstrap confidence intervals for the location of a quantitative trait locus. *Genetics*, 174(1), 481–489.

Marschner, H. (2012). *Mineral nutrition of higher plants* (3rd ed.). England: Elsevier.

McLaren, W., Gil, L., Hunt, S. E., Riat, H. S., Ritchie, G. R. S., Thormann, A., ... Cunningham, F. (2016). The ensembl variant effect predictor. *Genome Biology*, 17, 122.

Meuwissen, T. H. E., Hayes, B. J., & Goddard, M. E. (2001). Prediction of total genetic value using genome-wide dense marker maps. *Genetics*, 157(4), 1819–1829.

Mori, S., & Nishizawa, N. (1987). Methionine as a dominant precursor of phytosiderophores in graminaceae plants. *The Japanese Society of Plant Physiologists*, 28(6), 1081–1092.

Neugebauer, K., Broadley, M. R., El-serehy, H. A., & George, T. S. (2018). Variation in the angiosperm ionome. *Physiologia Plantarum*, 163, 306–322.

R Development Core Team. (2016) R: A language and environment for statistical computing.

Romay, M. C., Millard, M. J., Glaubitz, J. C., Peiffer, J. A., Swarts, K. L., Casstevens, T. M., ... Gardner, C. A. (2013). Comprehensive genotyping of the USA national maize inbred seed bank. *Genome Biology*, 14, R55.

Salt, D. E., Baxter, I., & Lahner, B. (2008). Ionomics and the study of the plant ionome. *Annual Review of Plant Biology*, 59, 709–733.

Schaaf, G., Ludewig, U., Erenoglu, B. E., Mori, S., Kitahara, T., & Von Wiren, N. (2004). ZmYS1 functions as a proton-coupled symporter for phytosiderophore- and nicotianamine-chelated metals. *Journal of Biological Chemistry*, 279, 9091–9096.

Scheipl, F., Greven, S., & Küchenhoff, H. (2008). Size and power of tests for a zero random effect variance or polynomial regression in additive

and linear mixed models. *Computational Statistics and Data Analysis*, *52*(7), 3283–3299.

Shakoor, N., Ziegler, G., Dilkes, B. P., Brenton, Z., Boyles, R., Connolly, E. L., ... Baxter, I. R. (2016). Integration of experiments across diverse environments identifies the genetic determinants of variation in *Sorghum bicolor* seed element composition. *Plant Physiology*, *170*, 01971.

Shi, R., Melzer, M., Zheng, S., Benke, A., Stich, B., & Von Wiren, N. (2018). Iron retention in root hemicelluloses causes genotypic variability in the tolerance to iron deficiency-induced chlorosis in maize. *Frontiers in Plant Science*, *9*, 557.

Shi, R., Weber, G., Köster, J., Reza-Hajirezaei, M., Zou, C., Zhang, F., & von Wiren, N. (2012). Senescence-induced iron mobilization in source leaves of barley (*Hordeum vulgare*) plants. *The New Phytologist*, *195*(2), 372–383.

Simić, D., Mladenović Drinić, S., Zdunić, Z., Jambrović, A., Ledenan, T., Brkić, J., ... Brkić, I. (2012). Quantitative trait loci for biofortification traits in maize grain. *Journal of Heredity*, *103*(1), 47–54.

Stangoulis, J. C. R., Huynh, B. L., Welch, R. M., Choi, E. Y., & Graham, R. D. (2007). Quantitative trait loci for phytate in rice grain and their relationship with grain micronutrient content. *Euphytica*, *154*(3), 289–294.

Stein, R. J., Höreth, S., de Melo, J. R. F., Syllwasschy, L., Lee, G., Garbin, M. L., ... Krämer, U. (2017). Relationships between soil and leaf mineral composition are element-specific, environment-dependent and geographically structured in the emerging model *Arabidopsis halleri*. *New Phytologist*, *213*, 1274–1286.

Tomatsu, H., Takano, J., Takahashi, H., Watanabe-Takahashi, A., Shibagaki, N., & Fujiwara, T. (2007). An *Arabidopsis thaliana* high-affinity molybdate transporter required for efficient uptake of molybdate from soil. *Proceedings of the National Academy of Sciences*, *104* (47), 18807–18812.

Urbany, C., Benke, A., Marsian, J., Huettel, B., Reinhardt, R., & Stich, B. (2013). Ups and downs of a transcriptional landscape shape iron deficiency associated chlorosis of the maize inbreds B73 and Mo17. *BMC Plant Biology*, *13*, 213.

Utz, H. F., Melchinger, A. E., & Schön, C. C. (2000). Bias and sampling error of the estimated proportion of genotypic variance explained by quantitative trait loci determined from experimental data in maize using cross validation and validation with independent samples. *Genetics*, *154*(4), 1839–1849.

VanRaden, P., Van Tassell, C., Wiggans, G., Sonstegard, T., Schnabel, R., Taylor, J., & 756 Schenkel, F. (2009). Reliability of genomic predictions for north American Holstein bulls. *Journal of Dairy Science*, *92*(1), 16–24.

von Wiren, N., Marschner, H., & Römheld, V. (1996). Roots of iron-efficient maize also absorb phytosiderophore-chelated zinc. *Plant Physiology*, *111*(4), 1119–1125.

Vreugdenhil, D., Aarts, M. G. M., Koornneef, M., Nelissen, H., & Ernst, W. H. O. (2004). Natural variation and QTL analysis for cationic mineral content in seeds of *Arabidopsis thaliana*. *Plant, Cell and Environment*, *27*, 828–839.

Wallace, J. G., Rodgers-Melnick, E., & Buckler, E. S. (2018). On the road to breeding 4.0: Unraveling the good, the bad, and the boring of crop quantitative genomics. *Annual Review of Genetics*, *52*(1), 421–444.

Waters, B. M., & Grusak, M. A. (2008). Quantitative trait locus mapping for seed mineral concentration in two *Arabidopsis thaliana* recombinant inbred populations. *New Phytologist*, *179*(4), 1033–1047.

White, P. J., Broadley, M. R., El-Serehy, H. A., George, T. S., & Neugebauer, K. (2018). Linear relationships between shoot magnesium and calcium concentrations among angiosperm species are associated with cell wall chemistry. *Annals of Botany*, *122*, 221–226.

Zhao, H., Sun, Z., Wang, J., Huang, H., Kocher, J. P., & Wang, L. (2014). CrossMap: A versatile tool for coordinate conversion between genome assemblies. *Bioinformatics*, *30*(7), 1006–1007.

Zhao, X., Luo, L., Cao, Y., Liu, Y., Li, Y., Wu, W., ... Lin, H. (2018). Genome-wide association analysis and QTL mapping reveal the genetic control of cadmium accumulation in maize leaf. *BMC Genomics*, *19*(1), 1–13.

Zheng, L., Huang, F., Narsai, R., Wu, J., Giraud, E., He, F., ... Shou, H. (2009). Physiological and transcriptome analysis of iron and phosphorus interaction in rice seedlings. *Plant Physiology*, *151*(1), 262–274.

SUPPORTING INFORMATION

Additional supporting information may be found online in the Supporting Information section at the end of this article.